16th World Conference on Earthquake, 16WCEE 2017

Santiago Chile, January 9th to 13th 2017

Paper N° 4206

Registration Code: S-T1466168968

PERFORMANCE AND SEISMIC VULNERABILITY OF A TYPICAL CONFINED MASONRY HOUSE IN CUENCA-ECUADOR

H. García[(1)], G. Degrande[(2)]

[(1)] *PhD student, Department of Civil Engineering KU Leuven-Belgium, hernan.garcia@kuleuven.be*
[(2)] *Professor, Department of Civil Engineering KU Leuven-Belgium, geert.degrande@kuleuven.be*

Abstract

The extent of damage in a city, in case of strong earthquakes, can be estimated from the results of the seismic vulnerability of its most common construction type. The aim of the present contribution is to determine the seismic vulnerability of a confined masonry building typical of Cuenca, Ecuador. Firstly, the macroscopic properties of masonry are derived from mesoscopic finite analyses of masonry piers. Secondly, the proposed structure is modeled using an equivalent frame method, in which masonry walls are defined as piers or spandrels using a macroelement model. Thirdly, a pushover analysis is performed on the structure; the results of this analysis are used to define an equivalent SDOF system. The properties of the SDOF are used to calibrate a single-macroelement model that characterizes the cyclic behavior of the MDOF model. Both models are capable to reproduce in-plane shear and flexural failure modes. Finally, nonlinear dynamic analyses are performed on the single-macroelement system for different ground motions, which are obtained from natural records (SIMBAD data base) compatible with the Ecuadorian design spectrum for several PGA levels. The maximum displacement of each analysis is compared with defined limit states, the exceedance of a limit state is recorded and then fitted to a fragility function using the maximum likelihood procedure. The proposed methodology presents an option for seismic vulnerability, to use in scenarios where little data is available.

Keywords: Masonry, Confined masonry, Cuenca, Seismic vulnerability, Equivalent SDOF

1. Introduction

Ecuador lies on the eastern rim of the seismically active area of the Pacific Ring of Fire with the Nazca plate as the main source for tectonic earthquakes. In consequence there have been at least 38 earthquakes of magnitude 7 Mw or higher since 1541 and an estimated 80,000 people died as a result of those events.

Cuenca is the third largest city of Ecuador with a total population, according to the last census, of 505,600 inhabitants, of which 330,000 constitute the urban population. Cuenca is characterized by low rise masonry buildings (80% of all dwellings [1]). In the city's center, buildings are based on an European style with their own characteristics, mostly built with timber and adobe. In 1999, Cuenca's center was listed as a UNESCO World Heritage Trust site. In the surroundings of the city, the construction practice changed since the 1980s, from timber to reinforced concrete for confining elements and from adobe walls to brick or block masonry.

According to Ecuador's Geophysical Institute, Cuenca lies over an intermediate risk zone (PGA of 0.25 g on rock), and it has seen a number of earthquakes over the years in the 4.0 to 4.9 Mw range. However, the no history of recent destructive earthquakes and no information of important events, led to an incorrect construction practice. Moreover, most masonry buildings were constructed without quality control (self-construction) nor fulfilling all building standards. This, combined with little understanding of building performance and no recorded data on the occurrence of structural damage, results in high level of uncertainty for building performance. In consequence, a large scale vulnerability analysis of the city was undertaken in 1999, by the seismic network research group of the University of Cuenca [2, 1], showing a high probability of collapse of masonry buildings (Fig. 1).

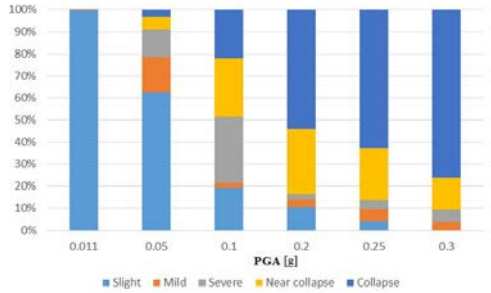

Fig. 1– Level of vulnerability of masonry buildings in the city of Cuenca [2,1] (adapted from [2]).

The aim of this paper is to present the seismic vulnerability of a typical two story confined masonry building, to compare with the result of previous study. Moreover, in order to present how materials characteristic can affect the strength of the structure, the building will be modeled using two types of brick. This study can be used to raise the concern in local authorities, which can implement a more rigorous control during planning and construction phases. Section 2 of this paper presents, the case study building and the modeling procedure. In Sections 3 the numerical solution used to evaluate seismic performance of the masonry structures is detailed. In section 4 the time history of displacements, due to selected ground motions, are obtained using a simplified model, which is able to approximate the cyclic response of the MDOF system. The maximum value of each analysis is compared with different performance levels. The vulnerability curves are fitted using the maximum likelihood analysis.

2. Case study building

2.1 Building description

Fig. 2 presents a two story confined masonry building. This structure is representative of typical housing in Cuenca, with living room and kitchen in the ground floor and bedrooms in the first story. The house presents also a garage and double pitched roof. The dwelling is part of the residential complex Laguna del Sol (325 dwellings) located at the east side at approximately 6 km from the city center. Each house is 6 m width, 9 m long and 6.4 m high.

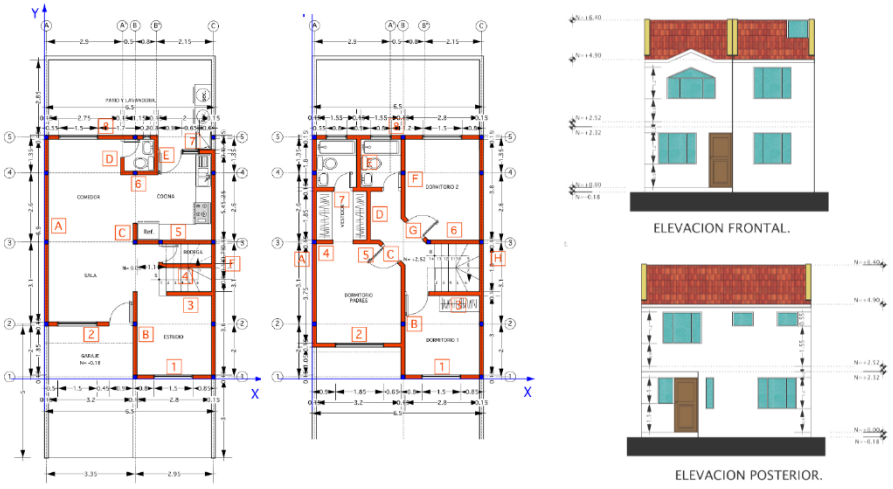

Fig. 2 – Architectural drawings of the prototype dwelling Laguna del Sol: plans and elevation views.

The building is composed of unreinforced masonry walls, reinforced concrete columns and beams; a 21 cm one-way concrete slab spans in the x direction. All masonry walls are 15 cm thick. The columns are 15 cm width and 20 cm depth; the beams are 15 cm width and 20 cm high. The foundation consists of a concrete strip footing constructed on a very dense soil or soft rock.

2.2. Building model and analysis

In this study the equivalent frame model, described in Lagomarsino & Penna [6] is used to estimate the in-plane response of the proposed structure to seismic loads (box-type behavior). The building is considered to be composed of frames, which, depending on the configuration of openings, are defined as piers or spandrels and rigid nodes. The identification and geometry of components follow a conventional criteria [6], which is supported from the damage survey after earthquakes and experimental campaigns. Piers are designated as elements carrying vertical and horizontal loads. Spandrels couple the response and modify the boundary of adjacent piers. Piers and spandrels are modeled using a one-dimensional macroelement [5], that is capable of representing flexural-rocking and shear behavior.

The macroelement model, defined by Penna [5], is ideally subdivided into three parts, two zero thickness interface elements with axial, compression and rotation degrees of freedom and one central part considered rigid (only shear deformation) with axial and rotation degrees of freedom. Relative displacement and rotation is allowed between the interface elements and the extremities of the central body. The initial elastic phase is determined by the elements axial, flexural and shear stiffness according to their geometric and mechanical properties. While for the inelastic phase nonlinear corrections terms, corresponding to cracking, toe-crushing and shear damage, modify the stiffness of the element.

Concrete beams and columns are modeled as 2D and 3D elements respectively. Their inelastic behavior is idealized by assuming elastic perfectly plastic hinges concentrated at the ends of the element. In the elastic phase the stiffness is determined by shear and flexural contribution, however reinforcement has no contribution to the stiffness. Shear, compressive/tensile failures are assumed as brittle, while combined axial force and bending moment as ductile. Shear strength is computed from to the criteria proposed in NTC 2008 and Eurocode 8 based on low-medium ductility classes. The formation of hinges for combined axial force and bending moment is determined by comparing the elastic prediction with limit values of the interaction diagram M-N, which is computed considering plane sections, perfect bond between concrete and steel bars and rectangular stress block distribution.

Floors are modeled using elastic orthotropic membrane finite elements (3 or 4 nodes) with two degrees of freedom at each node (u_x, u_y) in the global coordinate system. Floors are identified by a principal direction according to spanning orientation with Young's modulus E_1, a perpendicular direction with a Young's modulus E_2, Poisson ratio ν_{12} and shear modulus G_{12}. E_1 and E_2 represent the normal stiffness of the membrane along two perpendicular directions, affecting the degree of connection between walls and horizontal diaphragm and providing an horizontal displacement relation for nodes belonging to the same wall - floor intersection. G_{12} influences the tangential stiffness of the diaphragm, therefore the horizontal force transferred among walls.

2.3. Identification of mechanical characteristics

In case homogenized masonry panels, their properties are derived from mesoscopic finite element analyses of masonry piers consisting of bricks and mortar layers that are loaded in compression and shear, respectively.

The first analysis considers a masonry panel loaded in compression. Figure 3a shows a three-dimensional mesoscopic finite element model of a masonry panel consisting of five rows of two and a half bricks and mortar layers, bounded by two rigid steel beams. All components of this model are meshed using the eight-node hexahedron solid element with a maximum size equivalent to the width of a brick. The panel is fixed at the bottom, while the nodes at the top are constrained to move in the vertical direction. The masonry panel is loaded by a uniformly distributed uniaxial compressive load at the top steel beam.

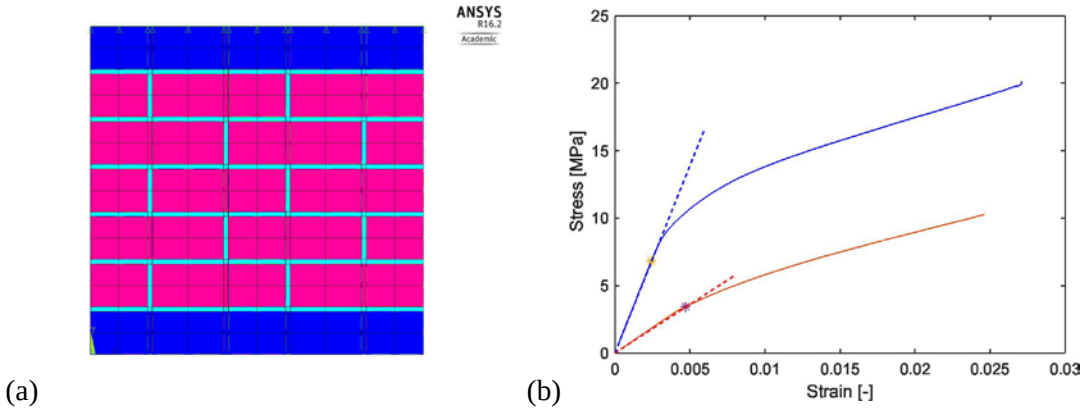

(a) (b)

Fig.3 - (a) Mesoscopic finite element model of a masonry panel consisting of ve rows of two and a half solid bricks (red) and mortar layers (light blue), bounded by two rigid steel beams (dark blue) and (b) stress-strain curve of a masonry panel consisting of hollow (red line) and solid (blue line) bricks under uniaxial compressive loading.

Table 1- Dimensions and average mechanical properties of hollow and solid bricks and mortar [4].

	l_b [m]	w_b [m]	h_b [m]	f_{cb} [MPa]	f_{tb} [MPa]	E_b [MPa]	G_b [MPa]
Hollow brick	0.30	0.13	0.20	2.77	0.098	709	284
Solid brick	0.28	0.14	0.09	8.3	0.3	3063	1225
	l_m [m]	w_m [m]	h_m [m]	f_{cm} [MPa]	f_{tm} [MPa]	E_m [MPa]	G_m [MPa]
Mortar	0.05	0.05	0.05	7.54	0.75	1508	603

The material characteristics of hollow and solid bricks, as well as mortar layers have been determined by means of laboratory testing at the University of Cuenca [4]. Table 1 summarizes the dimensions and the average compressive and tensile strength as well as the average Young's and shear modulus of hollow and solid bricks, as

determined by means of 22 compression tests on hollow bricks and 33 compression tests on solid bricks, together with characteristics of the mortar layer determined from 18 compression tests on 5 cm cubes. The cohesion and internal angle of friction of the bricks and mortar layer have been determined from their compressive and tensile strength. The non-linear behavior of these constituents is accounted for by means of a Drucker-Prager failure criterion that fits the Mohr-Coulomb criterion along the compression meridian. Fig. 3b shows the stress-strain curve of the masonry panel consisting of hollow and solid bricks, respectively, under compressive loading. Initially, the response is linear elastic (the tangent to the stress-strain curves is indicated in dashed lines on Fig. 3b) and the Young's modulus of the homogenized macroscopic masonry can be computed as:

$$E = \frac{E_b E_m (h_b + h_m)}{h_b E_m + h_m E_b} \quad (1)$$

where the thickness and the Young's modulus of the brick and mortar have been specified in Table 1. The Young's modulus of the hollow and solid brick masonry is equal to 727 MPa and 2777 MPa, respectively. From the stress-strain curves in Fig. 3b, the compressive strength f_m of the hollow and solid brick masonry is estimated the on-set of non-linear deformation as 3.44 MPa and 6.84 MPa, respectively.

The second analysis considers a masonry panel loaded in shear. Fig. 4a shows a three-dimensional mesoscopic finite element model of a masonry panel consisting of three rows of one brick and mortar layers, bounded by two rigid steel beams and three lateral rigid steel plates. All elements are meshed using the eight-node hexahedron solid element with a maximum size equivalent to a half of a brick. The panel at the bottom and the two left plates are fixed, while the nodes at the top are constrained to move in the vertical direction and the nodes in contact with the right plate are constrained to move in the horizontal direction. The masonry panel is loaded by a uniformly distributed uniaxial compressive load at the top steel beam and by a lateral uniformly distributed lateral load at the left steel plate.

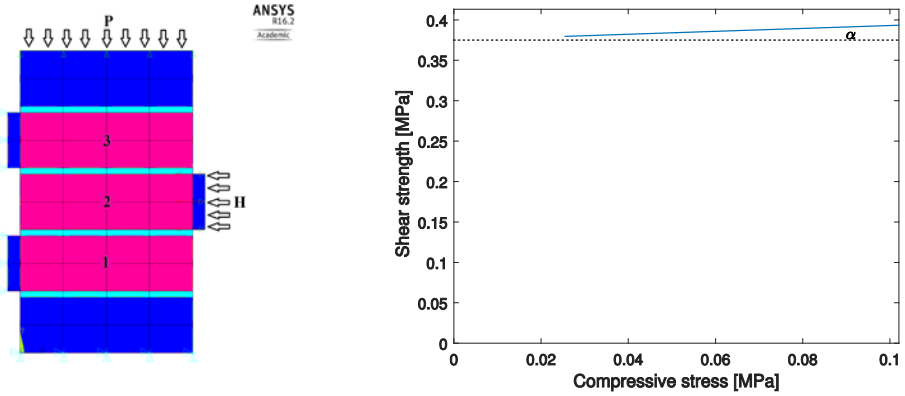

(a) (b)

Fig. 4 - (a) Shear-setup of finite element model based on solid bricks characteristics, (b) shear strength for different compression loads of finite element model based on solid bricks characteristics.

The material characteristics are the same as described previously and are summarized in Table 1. Figure 4b shows the shear strength curve for different compressive loads of the masonry panel consisting of solid bricks, this curve is defined by $f_{vi} = \frac{H}{2A}$ where H is the maximum shear force reached in the analysis, A is the cross-sectional area and f_{vi} the shear strength. The friction coefficient is defined as μ= tan (α), where α is represented in figure 4b. Table 2 summarizes all macroscopic properties of the homogenized masonry panel, which is composed with hollow and solid bricks respectively. For reinforced concrete columns and beams, the Young's modulus of concrete is estimated from $E_c = 4700\sqrt{f'_c}$ for a compressive strength of f'_c = 18 MPa [4], with a Poisson's coefficient v = 0.25. The reinforcement is based on a commonly used (in Ecuador) prefabricated steel cage (V5) composed with 9 mm main steel and 5.5 mm links every 150 mm with a yielding strength f_y = 500 MPa.

2.4. Model implementation

A 3D representation of the building is modeled using TREMURI [6]. A global Cartesian coordinate system (x, y, and z) is defined. The wall's vertical planes are determined based on the coordinates of one point (x, y) and the angle θ_z formed with the x axis. A complete explanation for the input of walls and elements is described in [7]. Fig. 5a shows the floor plans of the building; Fig. 5b shows the distribution of walls as implemented in TREMURI (11 walls, 7 parallel to the x and 4 parallel to the y axis).

Table 2- Summary of macroscopic properties for the homogenized masonry panel composed with hollow and solid bricks respectively.

	Young's modulus E [MPa]	Shear modulus G [MPa]	Density [kg=m^3]	Compressive strength f_m [MPa]	Cohesion f_{vo} [MPa]	Friction coefficient μ [-]
Hollow bricks	727	291	1600	3.44	0.091	0.13
Solid bricks	2777	1111	1800	6.84	0.3	0.145

Fig. 6 shows an example of three walls, composed of masonry panels, reinforced concrete elements (columns and beams) and openings, implemented in TREMURI. Macroelements will characterize piers (red) and spandrels (green), and simulate the in-plane response due to nonlinear static and dynamic forces. The behavior of masonry piers and spandrels is considered not to be affected by the interaction with the columns, however, an increase of ductility is expected as discussed in [8].

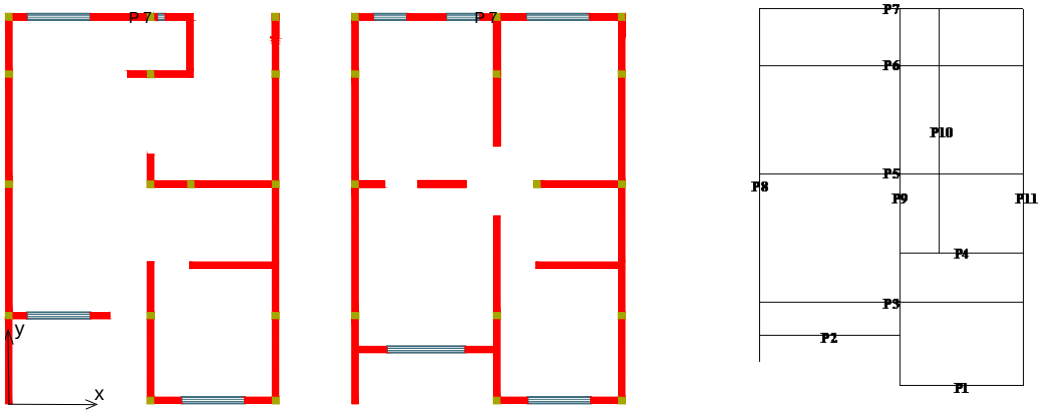

(a) (b)

Fig. 5 - (a) Ground floor and first floor masonry panels distribution, (b) walls definition a implemented in TREMURI.

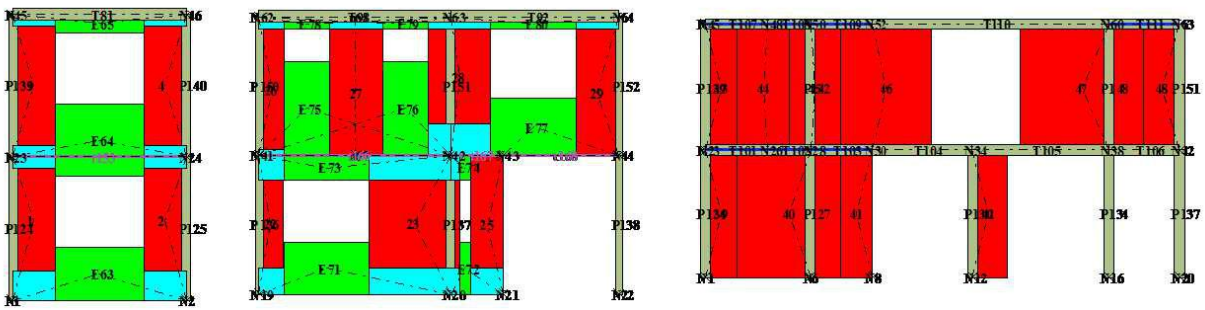

Fig. 6 - Example of walls using TREMURI for the proposed building (Fig. 5b): wall 1, wall 7 and wall 9 respectively.

3. Numerical solution

3.1. Natural vibration periods and modes

Figure 7 shows the first dominant lateral mode shape (x direction) of the models with masonry characteristics obtained from hollow and solid bricks respectively. The mass participating in the first mode of the former model the is 82%, while for the latter it is 83%.

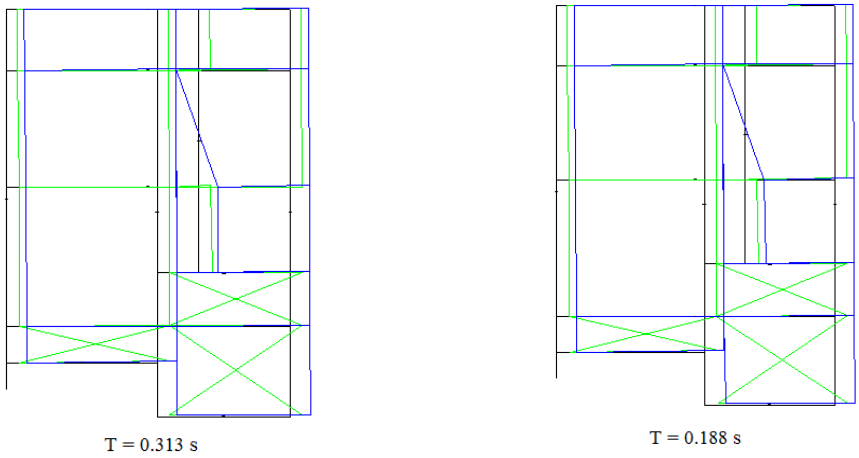

(a) (b)

Fig. 7 - First mode shape and period of the building with masonry characteristics obtained from: (a) hollow bricks and (b) solid bricks.

3.2. Pushover analysis

A displacement controlled pushover analysis is performed using an incremental invariant shape force (first mode shape). Firstly the control node at roof level is located in the center of gravity of the structure. Secondly the x direction is selected for the pushover analysis and the target displacement is set, finally base shear-force (F) and roof-displacement (D) at each force increment are obtained. Figure 8 shows the pushover curves (blue) for buildings composed of hollow and solid bricks.

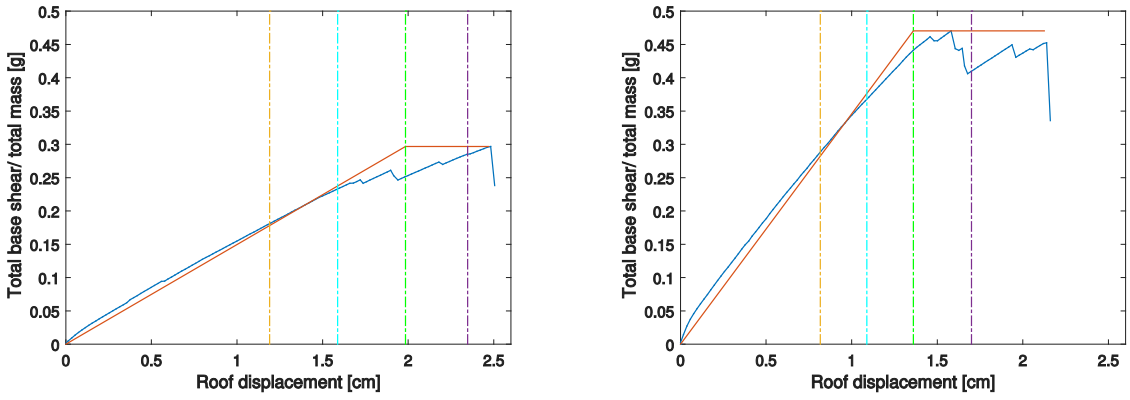

(a) (b)

Fig. 8 - Pushover curve (blue), equivalent bilinear approximation (red) and limits performance levels based on top roof displacement: fully operational (orange), operational (cyan), life safe (green) and near collapse (purple); for buildings composed of (a) hollow and (b) solid bricks.

In the initial phase, characterized by elastic behavior, the increment of load is mostly assumed by the walls. This phase is limited by a suddenly lost stiffness (intersection with cyan dotted line). Thereafter an increase of force produces stresses that exceed the capacity of masonry panels on different walls, starting with wall 7 (Fig. 9). The next stage is characterized by stiffness decay, since forces are redistributed through remaining bearing walls and reinforced concrete columns. This part presents a more ductile behavior, however with continuing presence of non-ductile failure from remaining masonry walls. Finally after an increment of force the building cannot withstand and total collapse happens (close to purple dotted line). The differences of the pushover analysis from both models are the increase of the overall stiffness due to improved masonry characteristics, and the decrease of ductility given by higher forces that produce more rapidly increase of stresses, exceeding the limit strength of remaining walls and concrete columns. In Fig. 9 is shown the stress condition of masonry panels and columns due to the last step of the pushover analysis, for the model with masonry properties obtained from hollow bricks. In the ground story, two masonry piers with insufficient robustness fail due to shear (yellow), two piers and a spandrel are in a shear plastic phase next to collapse (purple), one spandrel is in an inelastic phase (blue) and two reinforced columns (dark green) fail due to bending (crossed lines). In case of the first story, the masonry piers conforming the two small openings have more area to resist shear forces, therefore their level of stress is lower (inelastic phase), as consequence higher stresses are produced in the adjacent walls, thus the rest of masonry piers and spandrels are in a shear plastic phase (purple).

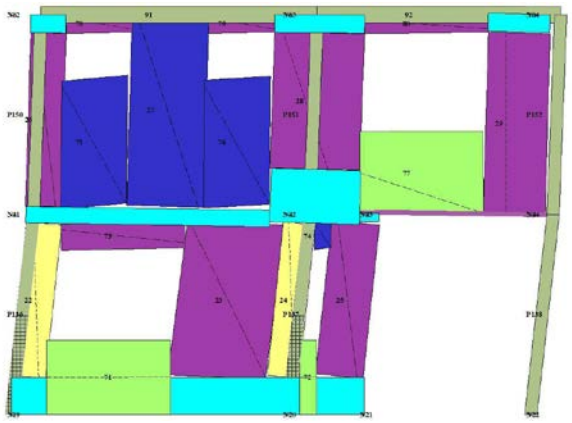

Fig. 9 - Final step of the pushover analysis of rigid nodes (cyan), elements in inelastic phase (blue), elements in shear plastic phase (purple) and elements in shear collapse (yellow) for wall number 7 of the building with hollow units.

3.3. Equivalent SDOF system

In practice simplified analysis based on displacement-based methods, e.g. [10, 11], are used for seismic assessment, however in this paper the roof displacement of the 3D model is estimated using an equivalent single-macroelement system, which is calibrated from an equivalent SDOF system. The advantages of the single-macroelement system are twofold; firstly the hysteretic behavior can be calibrated to represent the 3D model, secondly the simplified system is capable of modeling shear or flexural failure modes. Moreover existing methods can show inaccurate results for structures characterized by low first mode periods (< 0.5 s), which is in general the case of low rise confined masonry buildings. FEMA 440 presents results in which the response of an equivalent SDOF system with a period below 0.5 s, can either be, overestimated (Capacity spectrum method) or underestimated (Coefficient method).

The equivalent SDOF system is determined by calculating the first mode transformation factor Γ_1 using the methodology described in Eurocode 8. The values of Γ_1 for the proposed model with masonry characteristics from hollow and solid bricks are 1.38 and 1.30 respectively. Then the transformation to the SDOF system is determined by $F_n^* = \frac{F_n}{\Gamma_1}$ and $D_n^* = \frac{D_n}{\Gamma_1}$, where F_n and D_n are the shear force and target node displacement

respectively, at each time step. Fig.10 shows the transformation of the pushover to an equivalent SDOF system (red) and the bilinear approximation curve of the SDOF system (black).

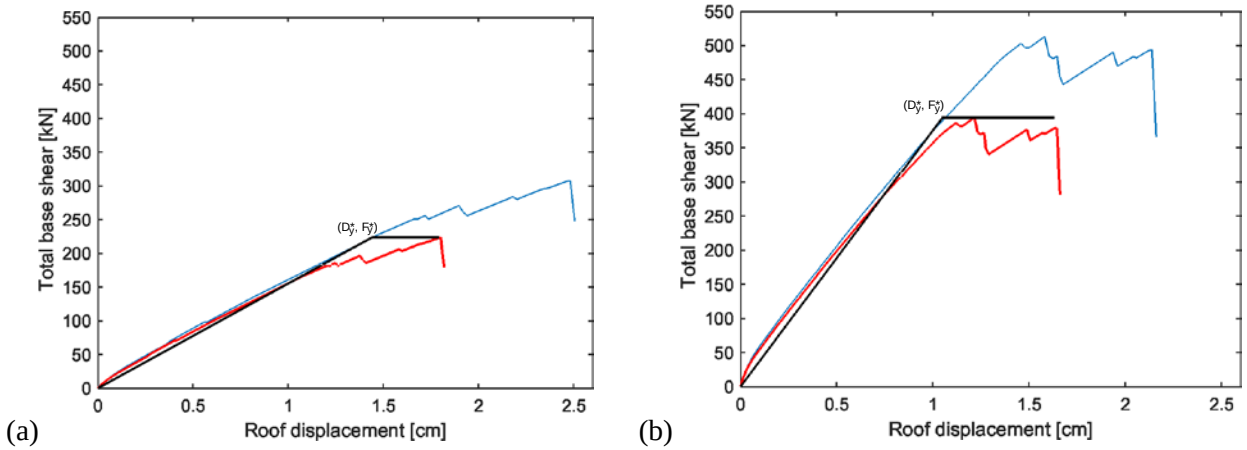

Fig. 10- The 3D model pushover curve (blue), F - D relation (red) and idealized elasto perfectly plastic F - D relation (black), for building with masonry characteristics obtained from (a) hollow and (b) solid bricks.

3.4. Single-macroelement

The single-macroelement model conserves the period and mass of the equivalent SDOF system. An initial element, assuming a height *h* and a thickness *s*, is given. The length *b* is obtained using

$$b = h\sqrt{\frac{\varsigma k^*}{Es}} \tag{2}$$

where ς is a calibration parameter initially equal to one. The length of the panel *b* is determined from a macroelement that accomplishes two conditions: firstly, it should satisfy $k' = k^*$, where k' is the stiffness after static condensation of the macroelement, which was created using the initial parameters. Secondly, it should describe a failure similar to the failure of the MDOF system. For the first condition, the stiffness of the macroelement k', defined in Penna and Lagomarsino [5], is compared with k^*. If k' is close within a tolerance range to k^*, *b* is accepted, otherwise *b* is recalculated using equation (2), this after updating ς defined as $\varsigma = \frac{k^*}{k'}$.

For the second condition, the pushover curve of the MDOF system is used to define a failure mode, which will characterize the type of failure for the single-macroelement model. If the failure is dominated by an axial-flexural behavior, then the macroelement should reach the maximum moment before failing in shear. On the other hand, if the failure is due to shear, then the wall should reach the maximum shear force before reaching the maximum moment. In this way it is possible to define, the compressive strength, friction coefficient and cohesion of the single-macroelement. The equations to estimate the parameters involved in this part of the calibration are obtained from the element constitutive model described in Penna [5] and from Mann & Muller [12].

Fig.11 presents the cyclic analysis of the MDOF and SDOF systems after calibration, showing good agreement between the simplified and 3D models, for target displacements below the collapse value (Fig. 8). The cyclic response presented in Fig. 11a corresponds to an element 0.89 m long, 1 m height and 0.4 m thick. On the other hand, Fig. 11b is the respond of an element 1.61 m long, 1 m height and 0.5 m thick. Both models show little degradation after each cycle, however in Fig. 11a the model presents less damage, this could be due to higher participation of the concrete columns before the failure of walls, contributing with ductility [13]. It is important to notice that these models behave properly for a certain range of displacements and drifts that are below the maximum recommended, presenting damage values in agreement with the reported damage in some masonry

buildings after an earthquake [14]. These results verify that the single-macroelement model can be a correct approximation of the MDOF system in estimate the seismic demands from different ground motions, using nonlinear dynamic analysis.

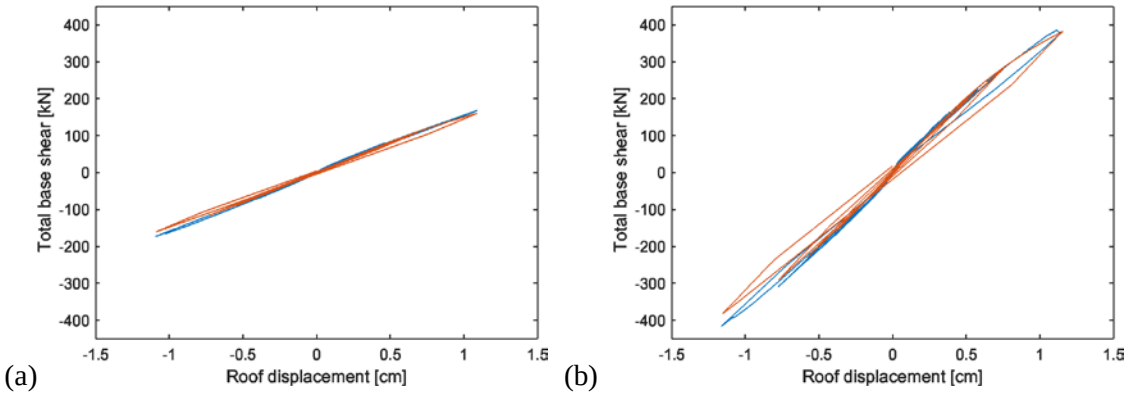

Fig. 11- Comparison of the force-displacement curves obtained from the pushover analysis in the X direction for the MDOF system (blue) and SDOF system (red) of a building with masonry characteristics obtained from (a) hollow and (b) solid bricks.

4. The Vulnerability analysis

The vulnerability is defined as the relation between hazard and structural capacity. For the former, the ground motions are selected from the SIMBAD data base using natural records compatible with the Ecuadorian design spectrum for the characteristics of Cuenca (Fig. 12), and for different PGA levels (from 0.05 g to 0.3 g) with a damping ratio of 5 % ; for this, the software REXEL is used [15].

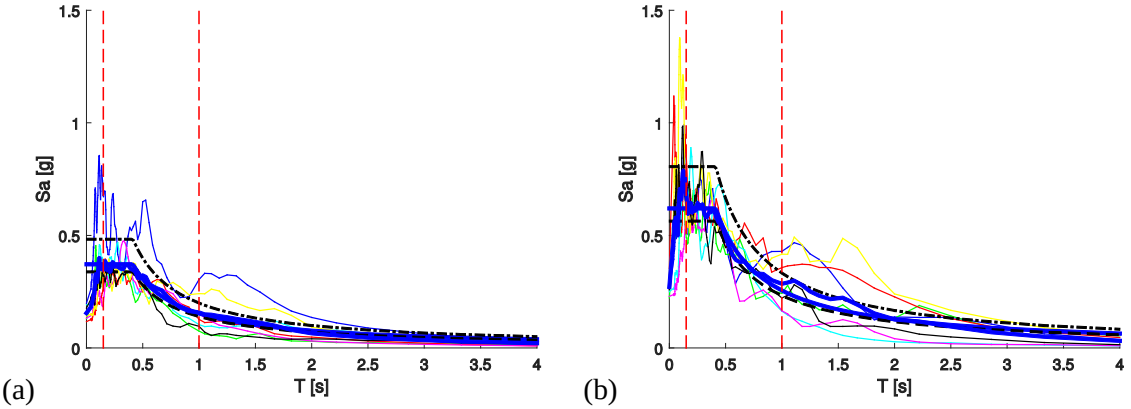

Fig. 12- Record selection based on Ecuador's design spectrum for PGA levels

(a) 0:15 g and (b) 0:25 g.

For the latter, nonlinear dynamic analyses were performed to the simplified model, using equivalent period, damping and mass. The lateral strength and hysteric behavior depend on the macroelement model based on the characteristics defined in the calibration. Fig. 8 shows the limit performance, for the pushover curve, for different limit states: fully operational (orange, 60% d_y), operational (cyan, 80% d_y), life safe (green, d_y) and near collapse (purple, d_u). Fig. 12 shows an example of 7 spectra of record selected for PGA levels 0.15 g and (b) 0.25 g according to the following parameters: Earthquakes from 4 - 7 M_w, soil type C (dense soils or soft rock $V_s \geq 760$ m/s) and records matching the design spectrum in the period range between 0.15 s and 1 s (red dashed line). Dynamic analyses, on the single-macroelement model, are performed using the records

corresponding to each PGA level. The maximum displacement is recorded and compared with the different limit states.

The statistical procedure for fitting the fragility functions is based on the Maximum Likelihood Estimation method (MLE) [16], which accounts for the non-constant variance of the observed fractions of collapse. The probability of observing z_j collapses out of n_j ground motions with PGA = x_j is given by the binomial distribution defined as

$$P(z_j \text{ collapses in } n_j \text{ ground motions}) = \binom{n_j}{z_j} p_j^{z_j} (1-p_j)^{n_j - z_j} \quad (3)$$

where P_j is the probability of a ground motion with PGA = x_j exceeding a limit performance point of the structure. The goal is to find the fragility function which best fits p, the MLE chooses the function with the highest probability of observing this limit state, considering all PGA values by taking the product of binomial probabilities at each PGA level.

Figure 13 shows the result of the vulnerability analysis of both models, in the case of the building with masonry characteristics obtained from hollow bricks for a PGA level of 0.25 g, the probability of collapse is > 95% (Fig. 13a), and for the building with masonry characteristics obtained from solid bricks for the same PGA level (Fig. 13b) the probability of collapse is approximately 30%.

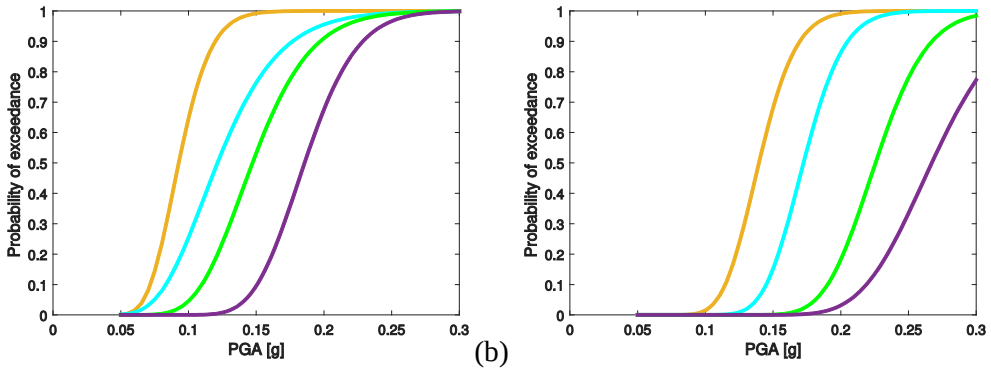

(a) (b)

Fig. 13- Limits performance levels defined on pushover curves based on top roof displacement: fully operational (orange), operational (cyan), life safe (green) and near collapse (purple); for buildings composed of (a) hollow bricks and (b) solid bricks.

5. Conclusions

A vulnerability analysis is presented for obtaining analytical fragility curves of a typical confined masonry house in Cuenca. This work was motivated due to the lack of research on this topology and by the presented results in the large scale vulnerability analysis. The selected building represents a typical construction type with great acceptation in the city.

The macroscopic properties of the homogenized masonry panels, were derived from mesoscopic finite element analyses of masonry panels consisting of bricks and mortar layers loaded in compression and shear, respectively. The mechanical definition of masonry defined the characteristics of the elements used in the 3D models based on an equivalent frame method, which was implemented in TREMURI, in which piers and spandrels were characterized as macroelements.

For the vulnerability analysis, it was necessary to define an equivalent SDOF system. This system was based one element macroelement, thus capable of modeling in-plane shear or flexural failure. The simplified model was subjected to a set of selected natural accelerograms using Ecuador's design spectra for different PGA levels.

The maximum displacement obtained from the nonlinear dynamic analysis of the simplified model, was compared with limit states defined in the pushover curve for the 3D model. Every demand exceeding a limit state was counted as collapse. Finally the fragility curves were plotted using the likelihood method.

The results presented are different to those obtained in the large scale vulnerability analysis, in which all masonry buildings were treated as unique with the same probability of collapse (60% and 70% for PGA levels of 0.25 g and 0.3 g respectively), showing that the level of vulnerability highly depends in the characteristic of materials. However, a high probability of collapse in the range of 0.25 g - 0.3 g is shown for buildings with masonry characteristics obtained from hollow bricks. Therefore, it is important to control the quality of materials before used in construction, this could make a difference in case of strong earthquakes. This maybe the reason of why certain buildings, with similar form, did not collapse in Pedernales and surroundings after the 7.8 Mw earthquake that strike on 16 April 2016.

Finally, this methodology can be extended to undertake the vulnerability analysis of Cuenca's buildings considering different topologies and materials.

6. Acknowledgements

This work is carried out with the support of SENESCYT and the University of Cuenca.

7. References

[1] J. Jiménez (2001): Vulnerabilidad sísmica de las edificaciones de la ciudad de cuenca mediante técnicas de simulación, in: Memorias de las XIVI Jornadas de Ingeniería Estructural.

[2] H. Bermeo, V. Loaiza (2001): Generación de escenarios de daño sísmico en la ciudad de Cuenca, Master' s thesis.

[3] D. Benedetti, G. Benzoni, M. Parisi (1988): Seismic vulnerability and risk evaluation for old urban nuclei, Earthquake Engineering and Structural Dynamics 16 183-201.

[4] F. Neira, L. Ojeda (1992): Dinteles de ladrillo armado, Master 's thesis.

[5] A. Penna, S. Lagomarsino, A. Galasco (2014): A nonlinear macroelement model for the seismic analysis of masonry buildings, Earthquake Engineering & Structural Dynamics 43, 159-179.

[6] S. Lagomarsino, A. Penna, A. Galasco, S. Cattari (2013) : Tremuri program: an equivalent frame model for the nonlinear seismic analysis of masonry buildings, Engineering Structures 56, 1787-1799.

[7] S. Lagomarsino, A. Galasco, A. Penna, S. Cattari (2008): TREMURI: Seismic Analysis Program for 3D Masonry Buildings (User Guide), Technical Report, Technical Report.(U. o. Genoa, Ed.) Genoa, Italy.

[8] M. Tomazevic (1999): Earthquake-resistant design of masonry buildings, volume 1, World Scientific.

[9] L. Gambarotta, S. Lagomarsino (1997): Damage models for the seismic response of brick masonry shear walls. part ii: the continuum model and its applications, Earthquake Engineering & Structural Dynamics 26, 441-462.

[10] S. A. Freeman, The capacity spectrum method as a tool for seismic design, in: Proceedings of the 11th European conference on earthquake engineering, Citeseer, pp. 6-11.

[11] P. Fajfar (2000): A nonlinear analysis method for performance-based seismic design, Earthquake spectra 16, 573-592.

[12] W. Mann, H. Muller, Failure of shear-stressed masonry. an enlarged theory, tests and application to shear walls, in: Proc. Br. Ceram. Soc., 30, p. 223.